

A Model Study of Turbidity Maxima in the York River Estuary, Virginia

JING LIN^{1*} and ALBERT Y. KUO²

¹ *School of Marine Science, College of William and Mary, Gloucester Point, Virginia 23062-1346*

² *Department of Bioenvironmental Systems Engineering, National Taiwan University, Taipei, Taiwan*

ABSTRACT: A three-dimensional numerical model is used to investigate the mechanisms that contribute to the formation of the turbidity maxima in the York River, Virginia (U.S.). The model reproduces the basic features in both salinity and total suspended sediments (TSS) fields for three different patterns. Both the prominent estuary turbidity maximum (ETM) and the newly discovered secondary turbidity maximum (STM) are simulated when river discharge is relatively low. At higher river inflow, the two turbidity maxima move closer to each other. During very high river discharge event, only the prominent turbidity maximum is simulated. Diagnostic model studies also suggest that bottom resuspension is an important source of TSS in both the ETM and the STM, and confirm the observed association between the turbidity maxima and the stratification patterns in the York River estuary. The ETM is usually located near the head of salt intrusion and the STM is often associated with a transition zone between upriver well mixed and downriver more stratified water columns. Analysis of the model results from the diagnostic studies indicates that the location of the ETM is well associated with the null point of bottom residual flow. Convergent bottom residual flow, as well as tidal asymmetry, is the most important mechanisms that contribute to the formation of the STM. The STM often exists in a region with landward decrease of bottom residual flow and net landward sediment flux due to tidal asymmetry. The channel depth of this region usually decreases sharply upriver. As channel depth decreases, vertical mixing increases and hence the water column is better mixed landward of the STM.

Introduction

Based on a two-year period of monthly slackwater surveys, Lin and Kuo (2001) found that in addition to the prominent estuarine turbidity maximum (ETM), a secondary turbidity maximum (STM) often exists in the middle reach of the York River, Virginia (Fig. 1). The STM was observed to move back and forth in the region of about 20 to 40 km from the York River mouth. The location of the STM was often associated with a transition zone between the upriver well-mixed and the downriver more stratified water columns. Relatively high bottom mud percentage and rapid sediment accumulation was reported in the region of the STM (Brown et al. 1938; Nichols et al. 1991; Dellapenna et al. 1998; Dellapenna 1999). A complete loss of transplanted eelgrass was observed after a month-long high turbidity pulse in the middle part of the York River estuary, and the decrease of seagrasses in this region was suggested to relate to the turbidity of the water column (Moore et al. 1997). A better understanding of the STM is not only relevant to the sediment transport issues in estuaries but also essential to the ecological systems in this region.

Much work has been done addressing the mechanisms of the ETM that are associated with the head of salt intrusion (Geyer 1993; Burchard and Baumert 1998). Little can be found that addresses the mechanisms of the STM, even though multiple peaks of bottom total suspended sediment (TSS) concentration have also been observed in several other estuaries (Roberts and Pierce 1976; Biggs et al. 1983; Dobereiner and McManus 1983; Weir and McManus 1987; Jay and Musiak 1994). Four mechanisms were identified as possible forming mechanisms of the STM through mathematical analysis (Lin 2001; Lin and Kuo 2001): bottom resuspension, convergence of bottom residual flow, tidal asymmetry, and inhibition of turbulence diffusion by stratification. There was not enough field data to substantiate any of the proposed mechanisms. Results from an intensive survey in the middle reach of the York River showed that TSS concentrations at southwestern shore stations were often much higher than those at the channel stations. The intra-tidal variation of the bottom TSS concentration was strongly related to the variation of bottom shear stress (Lin 2001). This suggests that a three-dimensional hydrodynamic-sediment model, which incorporates an intra-tidal time scale of sediment resuspension, would be essential in simulating the turbidity maxima in the York River estuary.

* Corresponding author: tele: 919/515-7767; fax: 919/515-7802; e-mail: jing_lin@ncsu.edu

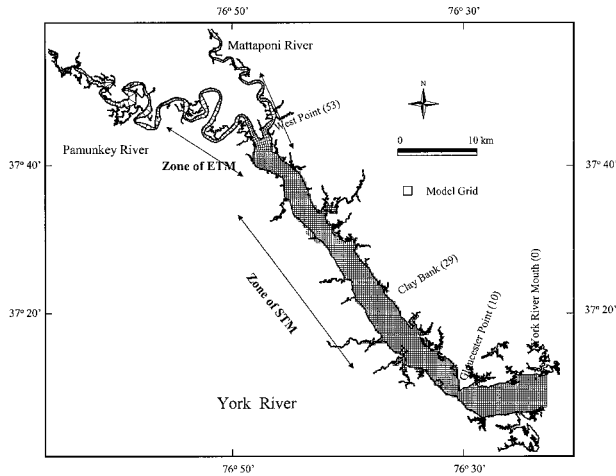


Fig. 1. HEM-3D York River model grid (the numbers inside parentheses indicate distances in km from York River mouth).

The objective of this paper is to investigate the potential mechanisms that contribute to the formation of the turbidity maxima using a numerical model. Since the organic composition in the TSS is small ($< 30\%$; Lin 2001; Lin and Kuo 2001), this paper only focuses on the hydrodynamic processes that contribute to the formation of the turbidity maxima in the York River. A description of the physical characteristics of the prototype estuary can be found in Lin and Kuo (2001).

Method

Virginia Institute of Marine Science (VIMS) three-dimensional Hydrodynamic-Eutrophication Model (HEM-3D; Park et al. 1995; Shen et al. 1998; Shen and Kuo 1999) is used to simulate sediment transport in the York River system. The hydrodynamic portion of HEM-3D is the Environmental Fluid Dynamics Code (EFDC) developed by Hamrick (1992, 1996). The model solves the Navier-Stokes equations for a domain with a free surface boundary condition using the vertically hydrostatic assumption. The model uses Mellor and Yamada's level 2.5 turbulence closure model (Mellor and Yamada 1982) modified by Galperin et al. (1988). Turbulent kinetic energy and turbulent length scale are solved using dynamically coupled transport equations. Sigma vertical coordinates and Cartesian or curvilinear-orthogonal horizontal coordinates are used in the model. Throughout the main stem of the York River, the horizontal resolution is 250 m. Varying grid sizes are used in the Pamunkey and Mattaponi Rivers (Fig. 1). The model has 8 vertical layers, which divide the local water depth equally.

The sediment transport model is coupled with

the hydrodynamic model with the same time resolution. The governing equation for the TSS concentration is

$$\frac{\partial C}{\partial t} + \frac{\partial C u}{\partial x} + \frac{\partial C v}{\partial y} + \frac{\partial C(w - w_s)}{\partial z} = \frac{\partial}{\partial x} \left(k_h \frac{\partial C}{\partial x} \right) + \frac{\partial}{\partial y} \left(k_h \frac{\partial C}{\partial y} \right) + \frac{\partial}{\partial z} \left(k_z \frac{\partial C}{\partial z} \right) \quad (1)$$

where C is the TSS concentration in the water column; x and y are the horizontal coordinates and z is the vertical coordinate positive upward; u , v , w are the water velocity components in x , y , z directions, respectively; w_s is the sediment settling velocity; and k_h and k_z are the horizontal and vertical turbulent diffusion coefficients, respectively.

At the water surface, no sediment flux is allowed, and the boundary condition is

$$w_s C + k_z \frac{\partial C}{\partial z} = 0 \quad (2)$$

The bottom boundary condition for sediment flux is

$$w_s C + k_z \frac{\partial C}{\partial z} = D - E \quad (3)$$

where E is the mass of sediment eroded from the bottom per unit bed area per unit time, also known as the erosion or resuspension rate; D is the mass of sediment deposited to the bottom per unit bed area per unit time, or the so-called deposition rate. The water contents of bottom sediments in the main stem of the York River vary from 60% to 80%, and the bottom sediments are mainly composed of silty clay (Nichols et al. 1991; Dellapenna 1999). The erosion rate for cohesive sediment is simulated as

$$E = \begin{cases} M \left(\frac{\tau_b}{\tau_{ec}} - 1 \right) & \text{for } \tau_b > \tau_{ec} \\ 0 & \text{for } \tau_b \leq \tau_{ec} \end{cases} \quad (4)$$

where τ_b is the bed shear stress, M is an empirical constant with the same units as E , and τ_{ec} is the critical shear stress for erosion.

The deposition rate D is calculated as $D = P w_s C_b$. P is the probability of deposition, of which different forms have been adopted by different modelers (McDonald and Cheng 1997; Sanford and Chang 1997). C_b is the sediment concentration near the bed. A commonly used formulation to define P is $P = (\tau_{dc} - \tau_b) / \tau_{dc}$ if bed shear stress is less than a critical shear stress for deposition (τ_{dc}) and $P = 0$ if the bottom shear stress is higher. The model calculates D as

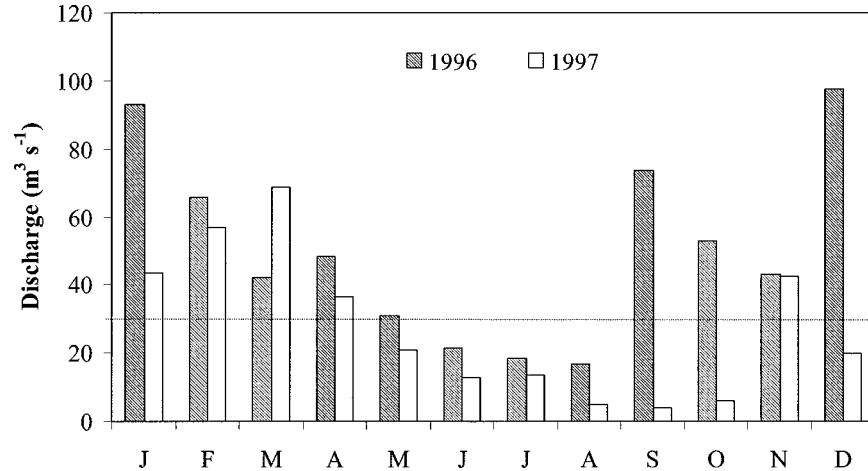


Fig. 2. Temporal variations of monthly mean freshwater discharges at upstream Pamunkey (data from USGS gauging station near Hanover, Virginia) in 1996–1997. The dotted line denotes a long-term (1942–2000) mean of the freshwater discharges.

$$D = \begin{cases} w_s C_b \frac{\tau_{dc} - \tau_b}{\tau_{dc}} & \text{for } \tau_{dc} > \tau_b \\ 0 & \text{for } \tau_{dc} \leq \tau_b \end{cases} \quad (5)$$

The model simulates one class of the cohesive sediments with sediment settling velocity calculated as

$$w_s = w_{s0} \times \left(\frac{C}{C_{ref}} \right)^{exp} \quad (6)$$

where w_{s0} is a reference sediment settling velocity, C_{ref} is a reference or normalizing sediment concentration; and exp is a dimensionless quantity. The dependence of sediment settling velocity on sediment concentration is to simulate the effect of flocculation. Since flocculation is not considered in this study, exp is set to zero, so that constant sediment settling velocity is used in this study. The major bottom sediment component in the upper and middle estuary is silty clay (Nichols et al. 1991). Suspended sediment comprising the turbidity maximum consists almost entirely of silt and clay with a mean size range of 2.6–3.2 μm from surface to bottom, and 2.2–2.8 μm with distance seaward through the turbidity maximum (Nichols and Thompson 1973). Nelson (1960) reported that the fine-grained sediment resists precipitation even in the very salty water obtained from the York River. He stated that the sediment distribution in the York River is determined primarily by the physical movement of water masses and current systems. We therefore used a low settling velocity of $5 \times 10^{-5} \text{ m s}^{-1}$, a value corresponding to fine silt without aggregation.

At the open boundary, tidal elevation data obtained from the National Oceanic and Atmospheric Administration database were used in prototype

simulations. During the flood tide, vertical distributions of salinity and suspended sediment concentration were estimated through linear interpolation in time between slackwater survey data from VIMS and data collected by the Chesapeake Bay Program. During the ebb tide, the salinity and sediment concentrations at the river mouth were determined from those inside the river assuming a frozen pattern, i.e., by advection without diffusion. As the tide changes from ebb to flood, the salinity and sediment concentrations were allowed to change linearly to the flood tide values over a specified time delay. The time period of delay is determined through calibration of salinity in hydrodynamic model.

At the upriver end of the model, two U.S. Geological Survey gauging stations, one on the Pamunkey River and the other on the Mattaponi River, provided the daily freshwater discharges. The patterns of seasonal river flow are represented in Fig. 2. There was not enough data of suspended sediment concentrations at the upriver end of the Pamunkey and Mattaponi Rivers. A seven-parameter log-linear regression model used in estimating loads of water quality constituents in tributaries of Chesapeake Bay (Cohn et al. 1992; Belval et al. 1994) was selected to estimate the suspended sediment concentrations introduced at the upriver ends. The parameters of the regression model were determined from historical data when TSS was monitored bi-weekly (1974–1994) and then were used for the prediction of TSS based on information of river discharge and the time of the year. The regression of the historical data gave a value of R^2 of 0.6. The concentration of the predicted TSS mainly varied from 5 to 100 mg l^{-1} .

A bed sediment model in the HEM-3D keeps

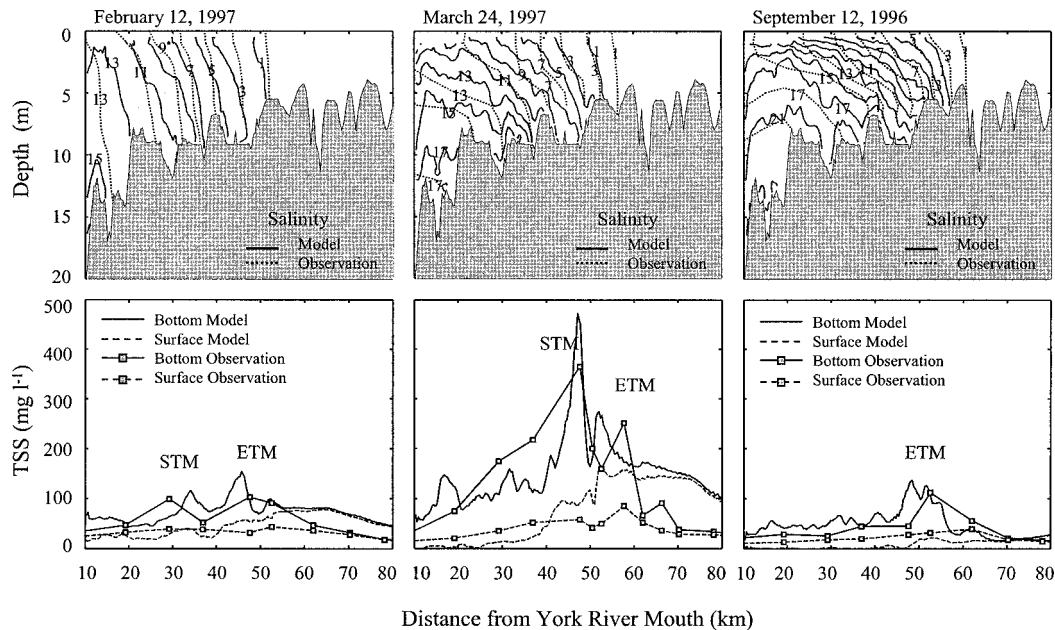


Fig. 3. Salinity (model results: solid line; survey data: dashed line) and TSS (model results of bottom TSS: solid line; surface TSS: dashed line; survey data of bottom TSS: solid line connected with \square ; surface TSS: dashed line connected with \square) distributions along the York-Pamunkey Rivers at slack before flood on February 12, 1997, March 24, 1997, and September 12, 1996, with unlimited bed sediment supply.

track of the net deposited sediment mass at the bed of each cell of the model grid. The sediment resuspension can be limited by the amount of the sediments at the bed. This feature is used in the diagnostic model studies described later.

The HEM-3D model for the York River system has been calibrated in terms of tidal behavior and salinity distributions (Sisson et al. 1997; Shen et al. 1998). The coupled sediment model is used in this study mainly for diagnostic purposes. Constant values of the empirical parameters ($M = 0.0005 \text{ g m}^{-2} \text{ s}^{-1}$; $\tau_{ec} = 0.1 \text{ Pa}$; $\tau_{dc} = 0.035 \text{ Pa}$; and $w_{s0} = 5 \times 10^{-5} \text{ m s}^{-1}$) are used within the model domain. The values of the parameters are selected through the calibration process of the prototype simulations.

Results

PROTOTYPE SIMULATIONS

Three periods were selected from the slackwater survey results to represent different TSS distribution patterns in the middle part of the York River (Fig. 3). A February 12, 1997, survey showed two distinct bottom TSS peaks: one associated with the head of salt intrusion and the other downstream where the water column was partially stratified. The freshwater discharge at upstream Pamunkey was $54.9 \text{ m}^3 \text{ s}^{-1}$ with a former peak discharge of $70.2 \text{ m}^3 \text{ s}^{-1}$ on February 10, 1997. A subsequent survey on March 24, 1997, showed that two TSS

peaks were very close and the water column was more stratified. Although the freshwater discharge at upstream Pamunkey ($48.1 \text{ m}^3 \text{ s}^{-1}$) was a little less than that on February 12, 1997, the former peak discharge was higher ($142.7 \text{ m}^3 \text{ s}^{-1}$ on March 21, 1997). The result from the slackwater survey on September 12, 1996, was chosen to represent the case that only one TSS peak was observed that was associated with the head of salt intrusion. Both the freshwater discharge on September 12, 1996, ($195.7 \text{ m}^3 \text{ s}^{-1}$) and the previous peak discharge on September 9, 1996, ($379.4 \text{ m}^3 \text{ s}^{-1}$) were the highest among the three cases.

The suspended sediment concentration was initialized to 20 mg l^{-1} within the model domain. Unlimited sediment source was specified at the bed. For the February 12, 1997, simulation, the model started on January 1, 1997, to accommodate the time needed to reach equilibrium from the zero initial condition of velocity and tidal height. The initial condition for salinity was based on the slackwater survey data on January 16, 1997, and held unchanged until simulation reached that date. The initial condition for the March 24, 1997, simulation run was from the February 12, 1997, simulation. The simulation period spanned August 1–September 12, 1996, for the third case and the initial condition of salinity was based on the slackwater survey data on August 7, 1996.

For the three prototype model simulations, the

model results roughly agree with the survey data in both salinity and TSS distributions (Fig. 3). The model reproduced the transition between upstream well-mixed to downstream more stratified water columns on February 12 and March 24, 1997, and the moderate stratification throughout the estuary on September 12, 1996. The model results are slightly over-stratified at the surface. Turbulence introduced from wind waves was not included in the simulation, which might contribute to the slight over-stratification. The Mellor and Yamada 2.5 turbulence closure model tends to underestimate turbulent mixing in the presence of stratification (Stacey et al. 1999). The head of salt intrusion simulated by the model was located seaward to that of the survey data. It took around 3 h for the vessel survey to reach West Point and about 2.5 h for the tide to propagate there. The discrepancy (between model and field data) of the salt intrusion in the upper portion of the estuary may have been partially caused by the difference of the time lag of the tidal propagation and the duration of the slackwater surveys.

The model also reproduced the two peaks of bottom TSS on February 12 and March 24, 1997, and the one peak on September 12, 1996. The model results of surface TSS concentration tend to be higher than the measurements at the upriver part of the estuary and lower at the seaward part. This may be due to the assumption that unlimited sediment source exists at the bed throughout the model domain. Upriver of West Point, a nodal point of tidal propagation exists in the Pamunkey River, where bottom tidal current is very strong. This results in high bottom shear stress, which leads to a high sediment resuspension rate in this region. Turbulence is not inhibited by stratification upriver of the salt intrusion, and hence high TSS concentration is uniformly distributed in the water column. In the lower part of the estuary, the slightly over-predicted stratification may be the reason that the simulated surface TSS concentration tends to be lower than the survey data.

The model reproduction of the basic features of different TSS distribution patterns indicates that the mechanisms controlling the formation and the movement of the ETM and the STM are well represented in the model. This allows diagnostic analyses to be conducted to study the mechanisms that contribute to the formation of the turbidity maxima in the York River.

DIAGNOSTIC ANALYSIS

The goal of diagnostic analysis is to examine the model responses to different environmental conditions, and to estimate the role of individual

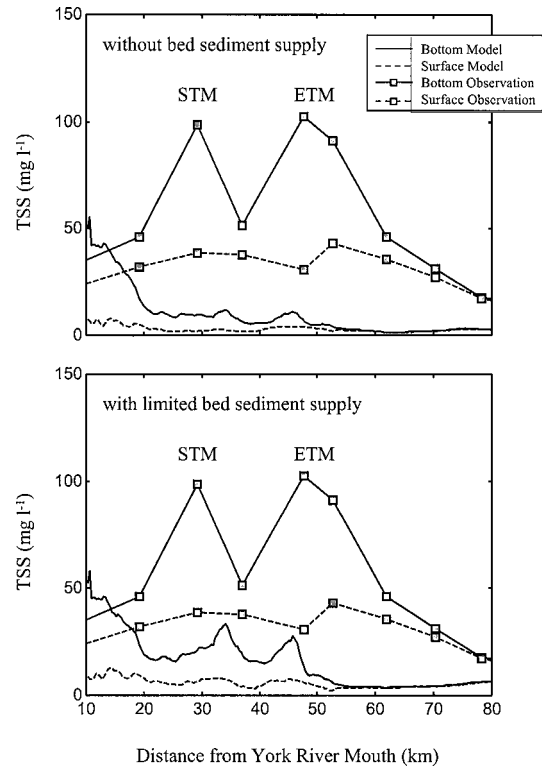


Fig. 4. TSS (model results of bottom TSS: solid line; surface TSS: dashed line; survey data of bottom TSS: solid line connected with \square ; surface TSS: dashed line connected with \square) distributions along the York-Pamunkey Rivers at slack before flood on February 12, 1997, without bed sediment supply and with limited bed sediment supply.

mechanisms that contribute to the TSS distribution features in the model domain.

The Importance of Bottom Sediment Resuspension

Data from the intensive survey showed that bottom resuspension may be an important source of the TSS in the middle reach of the York River (Lin 2001). Unlimited bed sediment supply was used in the three prototype simulations discussed above. In order to examine the importance of bed sediment supply to the formation of the STM, two additional model runs were made for the case of February 12, 1997.

In the first model run, zero bed sediment supply was used, which means that no bed sediment resuspension was allowed during the simulation period. In this case, if there were any turbidity maximum in existence, it would be purely due to convergence of sediment fluxes through water column processes and the sediment sources would be from freshwater input or from the marine side.

Fig. 4 shows the comparison between model results and the survey data of TSS distributions along the York River. Except close to the boundary,

where TSS concentration was specified according to observation data, the simulated TSS concentration in most of the model domain is only about 10% of that shown by the field data. The two peaks of the bottom TSS concentration were hardly noticeable.

In the second diagnostic test, limited bed sediment supply was specified as follows. The model starts from January 1, 1997, with bed sediment deposit initialized to zero. Both deposition and resuspension were activated so that the inventory of bed sediment was the deposited sediment from the water column during the simulation period.

Model results show that TSS concentration is much lower than the observation data. Two peaks of bottom TSS concentration did manifest in the middle to upper part of the estuary (Fig. 4). By including the resuspension process, both the ETM and the STM were reproduced by the model with a lower magnitude. This suggests that bottom sediment resuspension is a very important sediment source to the formation of both the ETM and the STM. The amount of bed sediment supply is crucial to the magnitude of the ETM and the STM.

Influence of River Discharges

Data from slackwater surveys suggest a close association of the stratification pattern in the York River and the location of the STM (Lin 2001; Lin and Kuo 2001). Since stratification is mainly affected by freshwater inflows, diagnostic model studies were conducted to examine the responses of the TSS field to different freshwater inflow conditions.

The model runs were driven by a tidal elevation time series using only the M_2 constituent, and constant freshwater discharge was specified for each case. The high freshwater inflow case (Pamunkey: $99.39 \text{ m}^3 \text{ s}^{-1}$; Mattaponi: $45.95 \text{ m}^3 \text{ s}^{-1}$) was determined as the discharge averaged over January, February, and March of 1997 and 1998 when the slackwater surveys were conducted. The constant freshwater discharge for the low flow condition (Pamunkey: $4.95 \text{ m}^3 \text{ s}^{-1}$; Mattaponi: $2.72 \text{ m}^3 \text{ s}^{-1}$) was determined as the discharge averaged over August, September, and October of 1997 when a continuous dry period was recorded. The model was run for 60 tidal cycles to reach steady state.

Under the high river inflow condition, only one bottom TSS peak (ETM) was simulated, which was associated with the head of salt intrusion around 50 km from the river mouth. Under the low river inflow condition, both the ETM and the STM persist over multiple tidal cycles, with the ETM associated with the head of salt intrusion and the STM in its seaward more stratified region (Fig. 5). This

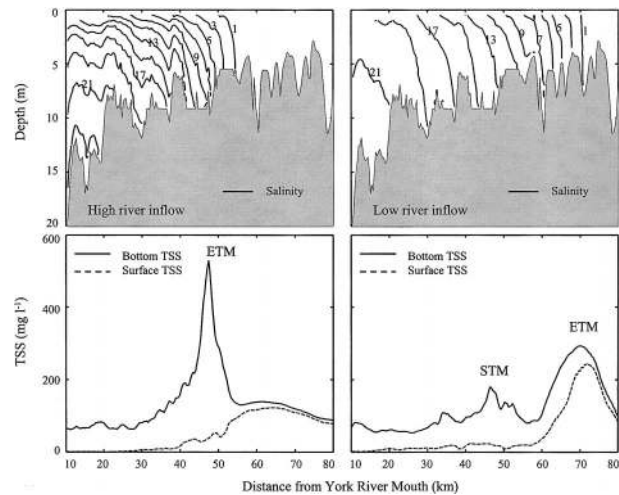


Fig. 5. Model results of tidally averaged salinity and TSS concentration distributions along the York-Pamunkey Rivers under high river inflow and low river inflow conditions.

confirmed the findings from the slackwater surveys (Lin 2001; Lin and Kuo 2001).

Influence of Spring-neap Tidal Cycle

In order to examine the influence of the spring-neap tidal variation on the TSS field in the York River system, both M_2 and S_2 tidal constituents were used in the forcing function at the open boundary. The mean tidal range at the mouth of the York River is around 0.7 m, and it could vary between 0.9 m and 0.5 m during spring and neap tides. At the river boundary, the constant high and low river discharge rates used in the second diagnostic study were applied.

Under the high river inflow condition, model results show that salinity intrudes a little farther during neap tide than during spring tide, which is due to the stronger vertical mixing and hence a weaker bottom residual flow during spring tide. The bottom TSS distribution shows that there is only one peak (ETM) existent throughout the 30 tidal cycle simulation period. This peak is located around 50 km from the river mouth, corresponding to the bottom 5‰ isohaline.

Under the low river inflow condition, salinity intrudes farther upriver, with the bottom 5‰ isohaline reaching above 60 km from the river mouth. The water column is well-mixed in most of the estuary. There are two peaks of bottom TSS concentration (the ETM and the STM). The ETM is located farther upriver than under the high river inflow condition with a slightly lower magnitude. The STM is located around 40–50 km from the river mouth with the magnitude higher during neap tide and lower during spring tide, which may

be due to a stronger convergence mechanism and weaker vertical mixing during neap tide.

ANALYSIS OF THE MECHANISMS

Using a two-dimensional approach, assuming steady state, integrating the mass balance equation over the bottom layer, and time averaging over a tidal cycle, Lin (2001) derived the following equation for the maintenance of the STM in the middle reach of the York River.

$$\frac{\partial \overline{C_b}}{\partial x} = -\frac{\overline{C_b}}{\overline{u_b}} \frac{\partial \overline{u_b}}{\partial x} - \frac{1}{\overline{u_b}} \frac{\partial \overline{u_b' C_b'}}{\partial x} - \frac{\text{flux}}{\overline{u_b} h_b} + \frac{\overline{E} - \overline{D}}{\overline{u_b} h_b} \quad (7)$$

where x is the distance along the channel and positive upriver, z is positive upward, and u is the velocity in x direction. The over bar indicates tidal mean, and the prime denotes the tidal deviation from the mean. Subscript b denotes values within a bottom layer where both the TSS concentration and the flow field can be represented by averaged values. The existence of the turbidity maximum is represented by positive $\partial \overline{C_b} / \partial x$ at the seaward side, zero at the peak concentration, and negative at the upriver side.

Four potential mechanisms were identified to cause and maintain the STM, which are represented by the four terms on the right hand side of Equation 7 respectively. They are: convergence of bottom residual flow (represented by the first term), tidal asymmetry (second term), inhibition of turbulence diffusion by stratification (third term), and local erosion (fourth term). The physical representations of the four terms in the equation were discussed in Lin (2001) and Lin and Kuo (2001). In addition to the four mechanisms, data from the intensive survey suggested that lateral sediment transport could contribute to the formation of the STM as well (Lin 2001). In order to discern the importance of each mechanism, an analysis of the model results for the above mechanisms follows.

Bottom Resuspension

The bottom sediment resuspension or erosion rate is calculated using Equation 4 in the model. The sediment resuspension rate is mainly controlled by bottom shear stress.

Model results from the diagnostic study for different river discharges (diagnostic study 2) show that, under both high and low flow conditions, three locations in the York River system have high bottom shear stress (Fig. 6). The first one corresponds to the nodal point of the tide in the Pamunkey River. The second one is located in the

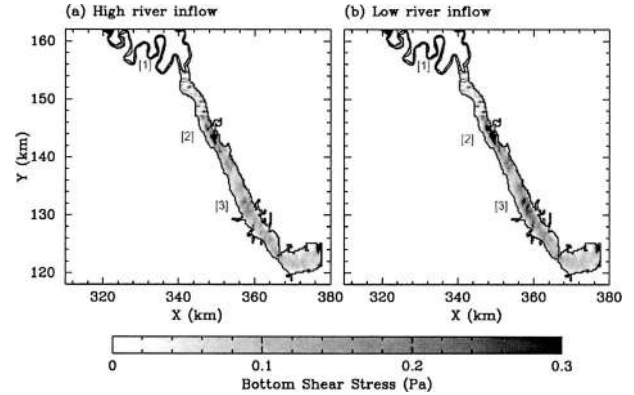


Fig. 6. Model results of spatial distributions of bottom shear stress under high river inflow and low river inflow conditions. The numbers in brackets denote places of high bottom shear stress.

middle to upper estuary of the York River, where the channel depth is shallow. The third high spot of bottom shear stress appears in the lower part of the York River, where the channel bifurcates and the main channel becomes much narrower moving upriver. Under the low river inflow condition, bottom shear stress is enhanced at the third location. The distribution of tidally averaged bottom TSS does not follow the distribution pattern of bottom shear stress. Under the high river inflow condition, only one bottom TSS peak (ETM) exists, which is located in the middle of the two upper high bottom shear stress regions. Under the low river inflow condition, the turbidity maximum separates into two peaks, with one (ETM) intruding farther upriver and the other (STM) moving seaward. The difference in the distribution patterns between the TSS and bottom shear stress indicates that although bottom resuspension is a major source of TSS in both the ETM and the STM, there are other mechanisms that control the locations of the ETM and the STM.

Convergence of Bottom Residual Flow

The formation of the ETM has been attributed to the convergence of bottom residual flow in most of the micro-tidal estuaries, although its role in the formation of the STM has not been established. Time series velocity outputs from the model (diagnostic study 2) were saved for stations along the York-Pamunkey River channels, and the principal axes were calculated for each station to get the along-channel velocity components. Since the model runs were driven by a tide using only the M2 constituent, the averages of the along-channel velocity components over one tidal cycle were calculated as the along-channel residual flow.

Fig. 7 shows the distribution of bottom residual

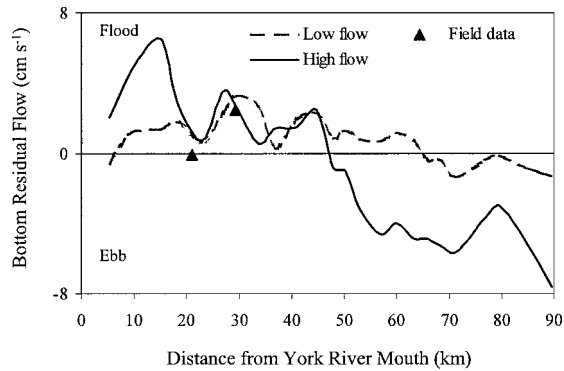


Fig. 7. Diagnostic model results of along-channel distributions of bottom residual flow under high and low river inflow conditions. Field data (\blacktriangle) is from a 13-h intensive survey on June 18, 1998.

flows along the York-Pamunkey River channels under the high and low river inflow conditions. There is a strong relationship between the flow conditions and the locations of the null point of the bottom residual flow. Under the high river inflow condition, the null point is located around 45–50 km from the river mouth. As freshwater inflow decreases, the null point moves farther upriver. Both are well associated with the locations of the ETM. This suggests that estuarine circulation, or convergence of bottom residual flow at the null point of the estuarine circulation is the major cause of the ETM in the York River system. Convergences not only occur around the null point where the bottom residual current changes direction, but also in regions with an upriver decrease of the strength of the residual flow. In addition to the null point of the estuarine circulation, there are two other regions (located around 15–22 and 30–35 km from the river mouth under the high river inflow condition, and also around 33–38 and 45–48 km from the river mouth under the low river inflow condition), which show convergent bottom residual flow. The simulated STM under the low river inflow condition resides around the second region of convergent bottom residual flow. In order to assess the importance of convergent bottom residual flow to the formation of both the ETM and the STM, velocity and TSS concentration output from the model were used to estimate $\bar{C}(\partial\bar{u}/\partial x)$ (indicated by the first term on the right-hand side of Equation 7) along the York-Pamunkey channels (Fig. 8). The distribution of $\bar{C}(\partial\bar{u}/\partial x)$ follows the variation pattern of residual flow. High (negative) peaks indicating strong convergence exist in the regions discussed above. All these sites are either near the head of salt intrusion or at locations where channel depth decreases rapidly upriver. Although the cross-sectional area decreases gradually upriver, the

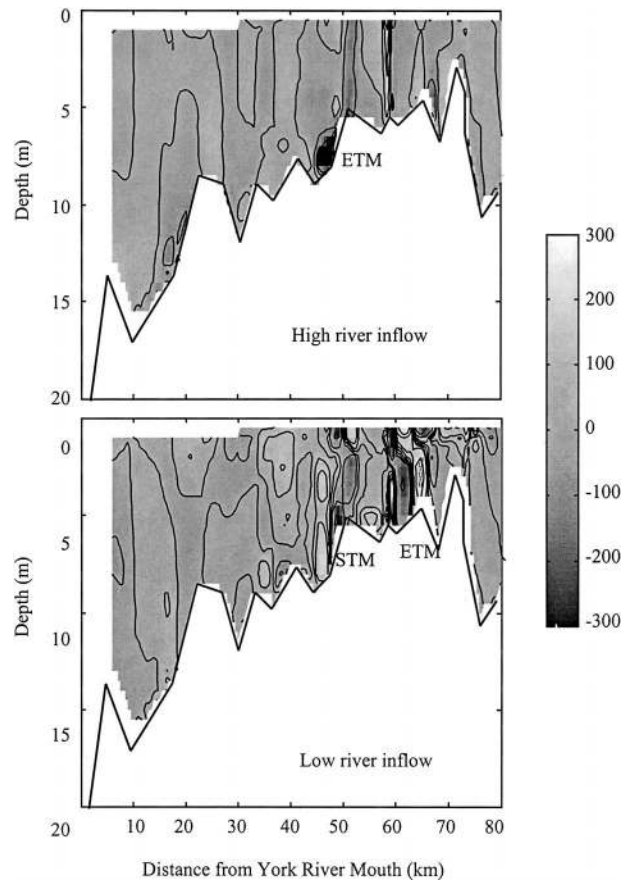


Fig. 8. Along-channel distributions of calculated $\bar{C}(\partial\bar{u}/\partial x)$ ($10^{-5} \text{ mg l}^{-1} \text{ s}^{-1}$) (x positive upriver, u is the velocity along x direction, C is the sediment concentration, and over bar denotes tidally mean) using model output under high river inflow and low river inflow conditions.

variation of channel depth is step-like (Fig. 9). The magnitude of bottom residual flow tends to decrease as channel depth decreases upriver. Convergent sediment transport is likely in regions where channel depth decreases rapidly upriver.

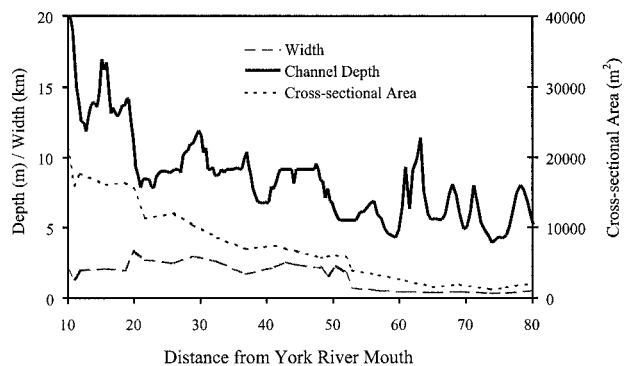


Fig. 9. Along-channel distributions of channel depth, cross-sectional area and river width of the York-Pamunkey Rivers.

Steady state was reached in the model diagnostic studies used in this analysis. According to Equation 7, if bottom residual flow is positive (upriver), the maintenance of turbidity maximum requires convergent sediment transport (negative gradient of bottom residual flow) at its seaward side and divergent sediment transport (positive gradient of bottom residual flow) at its upriver side. Fig. 8 shows that the ETM is located in such a region. The STM only occurs under the low river inflow condition, and it is associated with a region of decreasing bottom residual flow, where the channel depth decreases upriver. Although strong convergence of bottom residual flow also exists in the lower part of the York River (around 15–22 km from the river mouth) under the high river inflow condition, no STM occurs there.

Tidal Asymmetry

Tidal asymmetry is defined in this study as the non-linear interaction between the tidal flow and TSS variation over a tidal cycle. It can be caused by either the non-symmetrical distribution of TSS field over flood-ebb tidal cycle or, by the asymmetry of the tidal current itself. Much higher sediment concentration was observed during maximum flood than ebb (Friedrichs et al. 1999), possibly due to tidal straining (Simpson et al. 1990; Geyer 1993). In addition, flood currents tend to be bottom intensified and ebb currents tend to be surface intensified due to a stronger vertical mixing during flood tide and a stronger stratification during ebb tide (Jay and Musiak 1994). These could lead to a net landward sediment flux. In the upriver region of a well-mixed water column, little upriver sediment flux by this mechanism is expected, and hence a convergence of sediment fluxes could exist.

The gradient of sediment flux due to tidal asymmetry, $\partial C'u'/\partial x$ (indicated by the second term on the right-hand side of Equation 7), was plotted in Fig. 10. Convergent sediment transport was indicated by a negative value of $\partial C'u'/\partial x$, divergent sediment transport was indicated by a positive value. Under the high river inflow condition, strong convergence of sediment transport exists at about 50 km from the river mouth, where the ETM is located. Under the low river inflow condition, convergent sediment transport due to tidal asymmetry exists near the STM and the magnitude of the convergence is higher than that due to convergent residual flow. The STM does not appear at places where there is no convergent sediment flux due to tidal asymmetry, even though there is convergent bottom residual flow. This suggests that tidal asymmetry is a major factor in determining the location of the STM in the York River system.

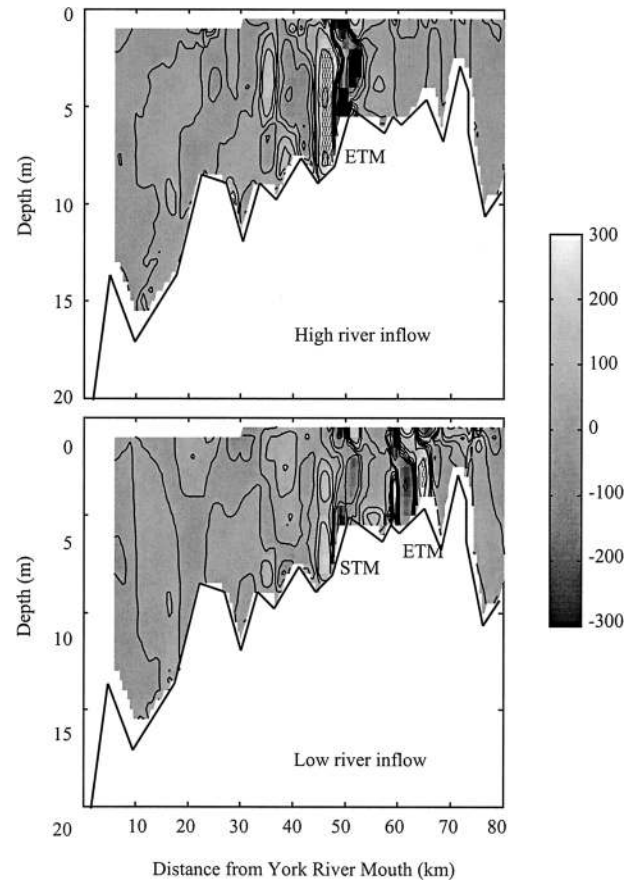


Fig. 10. Along-channel distribution of calculated $\partial \overline{C'u'}/\partial x$ ($10^{-5} \text{ mg l}^{-1} \text{ s}^{-1}$) (x positive upriver, u is the velocity along x direction, C is the sediment concentration, over bar denotes tidal mean, and prime indicates tidal deviation from the mean) using diagnostic model results under high river inflow and low river inflow conditions.

Time series of the model results of the flow velocity and TSS concentration at cells close to the STM and the ETM are examined under the low river inflow condition to show the along-channel variation of the sediment flux due to tidal asymmetry. Seaward of the STM, bottom shear stress is higher during flood than during ebb, which leads to more sediment resuspension into the water column during flood. During flood, high TSS concentration can reach a higher portion of the water column where velocity is stronger (Fig. 11). The asymmetrical distribution of TSS concentration may be caused by tidal straining, which could cause a more stratified water column during ebb than during flood. The asymmetry leads to a stronger upriver sediment flux during flood than the seaward sediment flux during ebb. Therefore, a net upriver sediment flux exists in this region.

At stations between the STM and the ETM, the magnitude of bottom shear stress is about the same

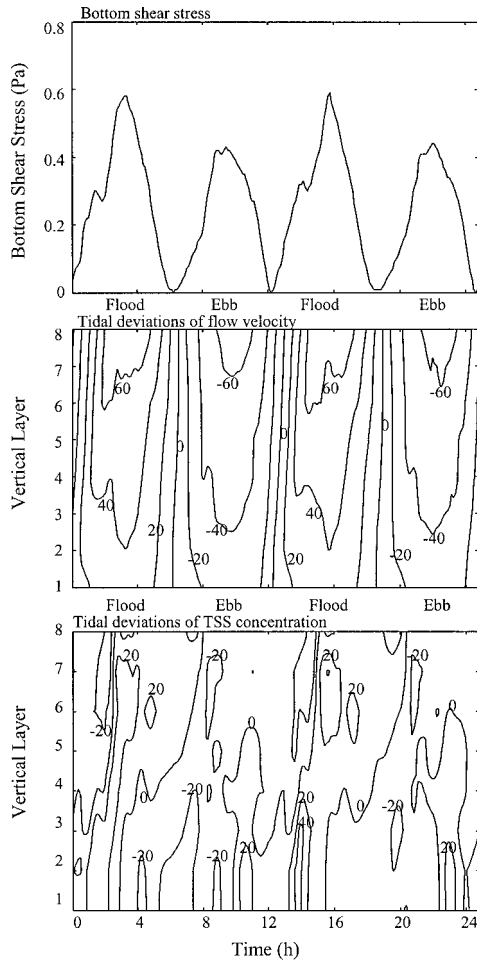


Fig. 11. Temporal distributions of bottom shear stress, tidal deviations of flow velocity (cm s^{-1}), and tidal deviations of TSS concentration (mg l^{-1}) at a channel cell about 40 km from the York River mouth (about 7 km downstream of the STM). Data are from diagnostic model studies with constant low river inflow condition.

during flood and during ebb. The signal of sediment advection appears much stronger than bottom resuspension. Instead of TSS peak concentration at maximum flow speed, high TSS concentration occurs close to slack before ebb (upriver of the STM) or slack before flood (seaward of the ETM). This suggests that the high TSS concentration is probably due to suspended sediment being advected from the STM (during flood to upriver of the STM) or the ETM (during ebb to seaward of the ETM). Upriver of the ETM, although the bottom shear stress is higher during flood than during ebb, the temporal variation of the TSS concentration is rather a response to the ETM than a cause. The TSS peak concentration occurs at slack before ebb due to advection from the ETM.

According to Simpson et al. (1990), the effect of

tidal straining is proportional to the water depth. As channel depth decreases upriver, the net upriver sediment flux decreases. This results in convergent sediment flux in the region where channel depth decreases sharply upriver. The association of the STM with the transition between the upriver well-mixed and the seaward more stratified water columns may be due to the fact that both are associated with a sharp upriver decrease in the water depth.

Inhibition of Turbulence Diffusion by Stratification

Sediment is kept in suspension by the upward turbulence diffusion. If turbulence is inhibited by stratification in the STM region, more resuspended sediment will be confined to near bottom. Coupled with the residual circulation, suspended sediment will be trapped in a transition zone between upriver well-mixed and seaward more stratified water columns. This mechanism is represented by the third term of Equation 7. As an indication of this mechanism, the TSS concentration should be more uniformly distributed at the upriver side of the STM and more confined to near bottom at the seaward side. Under the low river inflow condition, model results show that high TSS concentration are confined to near bottom at both the upriver and seaward sides of the STM, which suggests that this mechanism contributes little to the formation of the STM.

Lateral Sediment Transport

Data from an intensive survey suggested that lateral sediment transport is not a negligible sediment transport processes in the middle reach of the York River (Lin 2001). Tidally averaged lateral sediment flux was calculated from the model output data at a transect around 50 km from the river mouth, where the ETM located under the high river inflow condition and the STM located under the low river inflow condition. In the channel of the transect, weak convergence of lateral residual flow exists near the surface and weak divergence exists near the bottom. The magnitude of the convergence is much lower than that due to convergent residual flow.

Summary and Discussion

The most important result of this study is perhaps that the newly discovered STM in the York River system was simulated by a three-dimensional numerical model. The model results confirmed the relationship between different flow conditions and the occurrence of the STM. Convergent sediment fluxes due to tidal asymmetry as well as an upriver decrease of bottom residual flow may determine the location of the STM.

The model results suggest that bottom sediment resuspension is an important source of the TSS in both the ETM and the STM regions. Under the high river inflow condition, freshwater pushes the null point of estuarine circulation towards the middle part of the York River system. Strong convergence of upriver sediment fluxes due to tidal asymmetry occurs at the same place of the strengthened convergence of bottom residual flow. This results in a very high peak of bottom TSS concentration, the ETM. Under the low river inflow condition, as freshwater discharge diminishes, the ETM moves upriver with the null point of the estuarine circulation. The strong convergence of sediment fluxes due to tidal asymmetry remains at the middle part of the York River estuary, which combined with a smaller convergence of bottom residual flow, forms the secondary turbidity maximum.

There are some limitations of the sediment model used in this study that have to be considered and improved upon in future study. One class of suspended sediment was simulated in all the model runs. Constant values of critical shear stress for erosion, τ_{ec} , critical shear stress for deposition, τ_{dc} , and settling velocity, w_s , were applied over the entire model domain. Varying bed and suspended sediment size distributions were observed in the York River (Nichols et al. 1991; Dellapenna 1999). In-situ measurements indicated that τ_{ec} may vary with characteristics such as the sediment type, bioturbation of the bottom sediments, depth of the eroded material, or the existence of a fluff layer (Maa et al. 1993; Sanford and Maa 2001). The processes of flocculation and bed sediment consolidation were not simulated in this model study. The importance of these processes to the formation of the STM is not clear. The analysis of the model results in this study serves as a qualitative indication of the importance of each potential mechanism that contributes to the formation of the STM. For a more accurate simulation of the TSS distributions in the York River, the factors discussed above need to be considered in the model.

ACKNOWLEDGMENTS

The study described in this paper was partially supported by the Contaminant and Sediment Transport program of the Virginia Chesapeake Bay Initiatives. We would like to thank Mac Sisson for his help in proofreading the manuscript. We are grateful to Jian Shen and Harry Wang for their advice and comments on the handling of numerical models.

LITERATURE CITED

- BELVAL, D. L., M. D. WOODSIDE, AND J. P. CAMPBELL. 1994. Relation of stream quality to streamflow, and estimated loads of selected water-quality constituents in the James and Rappahannock Rivers near the fall line of Virginia, July 1988–June 1990. U.S. Geological Survey, Water-Resources Investigations Report 94-4042. U.S. Geological Survey, Denver, Colorado.
- BIGGS, R. B., J. H. SHARP, T. M. CHURCH, J. M. TRAMONTANO, AND J. WATSON. 1983. Optical properties, suspended sediments, and chemistry associated with the turbidity maxima of the Delaware estuary. *Canadian Journal of Fisheries and Aquatic Sciences* 40:172–179.
- BROWN, C. B., L. M. SEAVY, AND G. RITTENHOUSE. 1938. Investigation of silting in the York River, Virginia. Advanced report SCS-SS-32. U.S. Department of Agriculture, Soil Conservation Service, Washington, D.C.
- BURCHARD, H. AND H. BAUMERT. 1998. The formation of estuarine turbidity maxima due to density effects in the salt wedge. A hydrodynamic process study. *Journal of Physical Oceanography* 28:309–321.
- COHN, T. A., D. L. CAULDER, E. J. GILROY, L. D. ZYNJUK, AND R. M. SUMMERS. 1992. The validity of a simple statistical model for estimating fluvial constituent loads: An empirical study involving nutrient loads entering Chesapeake Bay. *Water Resources Research* 28:2353–2363.
- DELLAPENNA, T. M. 1999. Fine-scale strata formation in biologically and physically dominated estuarine systems within the lower Chesapeake and York River subestuary. Ph.D. Dissertation, Virginia Institute of Marine Science, The College of William and Mary, Gloucester Point, Virginia.
- DELLAPENNA, T. M., S. A. KUEHL, AND L. C. SCHAFFNER. 1998. Sea-bed mixing and particle residence times in biologically and physically dominated estuarine systems: A comparison of lower Chesapeake Bay and the York River subestuary. *Estuarine, Coastal and Shelf Science* 46:777–795.
- DOBEREINER, C. AND J. MCMANUS. 1983. Turbidity maximum migration and harbor siltation in the Tay estuary. *Canadian Journal of Fisheries and Aquatic Sciences* 40:117–129.
- FRIEDRICH, C. T., L. C. SCHAFFNER, T. M. DELLAPENNA, AND J. LIN. 1999. Migration of mud beds associated with double turbidity maxima in a tidally energetic, partially-mixed estuary, p. 37. In Abstract of ERF '99, The 15th Biennial International Conference. ERF, New Orleans, Louisiana.
- GALPERIN, B., L. H. KANTHA, S. HASSID, AND A. ROSATI. 1988. A quasi-equilibrium turbulent energy model for geophysical flows. *Journal of the Atmospheric Sciences* 45:55–62.
- GEYER, W. R. 1993. The importance of suppression of turbulence by stratification on the estuarine turbidity maximum. *Estuaries* 16:113–125.
- HAMRICK, J. M. 1992. A three-dimensional environmental fluid dynamics computer code: Theoretical and computational aspects. Special report on Marine Science and Ocean Engineering No. 317. Virginia Institute of Marine Science, The College of William and Mary, Gloucester Point, Virginia.
- HAMRICK, J. M. 1996. User's manual for the environmental fluid dynamics computer code. Special Report in Applied Marine Science and Ocean Engineering No. 331. Virginia Institute of Marine Science, The College of William and Mary, Gloucester Point, Virginia.
- JAY, D. A. AND J. D. MUSIAK. 1994. Particle trapping in estuary tidal flows. *Journal of Geophysical Research* 99:20445–20461.
- LIN, J. 2001. A study of the secondary turbidity maximum in the York River estuary, Virginia. Ph.D. Dissertation, Virginia Institute of Marine Science, The College of William and Mary, Gloucester Point, Virginia.
- LIN, J. AND A. Y. KUO. 2001. Secondary turbidity maximum in a partially mixed microtidal estuary. *Estuaries* 24:707–720.
- MAA, J. P.-Y., L. D. WRIGHT, C.-H. LEE, AND T. W. SHANNON. 1993. VIMS Sea Carousel: A field instrument for studying sediment transport, 1993. *Marine Geology* 115:271–287.
- MCDONALD, E. T. AND R. T. CHENG. 1997. A numerical model of sediment transport applied to San Francisco Bay. *Journal of Marine Environmental Engineering* 4:1–41.
- MELLOR, G. L. AND T. YAMADA. 1982. Development of a turbulence closure model for geophysical fluid problems. *Reviews of Geophysics and Space Physics* 20:851–875.

- MOORE, K. A., R. L. WETZEL, AND R. J. ORTH. 1997. Seasonal pulses of turbidity and their relations to eelgrass (*Zostera marina* L.) survival in an estuary. *Journal of Experimental Marine Biology and Ecology* 215:115–134.
- NELSON, B. W. 1960. Recent sediment studies in 1960. *Mineral Industries Journal* 7:1–4.
- NICHOLS, M. M., S.-C. KIM, AND C. M. BROUWER. 1991. Sediment characterization of the Chesapeake Bay and its tributaries. NOAA National Estuarine Inventory, Virginia Institute of Marine Science, The College of William and Mary, Gloucester Point, Virginia.
- NICHOLS, M. M. AND G. THOMPSON. 1973. Development of the turbidity maximum in a coastal plain estuary. Final Report for U.S. Army Research Office Durham, Virginia Institute of Marine Science, The College of William and Mary, Gloucester Point, Virginia.
- PARK, K., A. Y. KUO, J. SHEN, AND J. M. HAMRICK. 1995. A three-dimensional hydrodynamic-eutrophication model (HEM-3D): Description of water quality and sediment process submodels. Special report in Applied Marine Science and Ocean Engineering No. 327. Virginia Institute of Marine Science, The College of William and Mary, Gloucester Point, Virginia.
- ROBERTS, W. P. AND J. W. PIERCE. 1976. Deposition in upper Patuxent estuary, Maryland, 1968–1969. *Estuarine and Coastal Marine Science* 4:267–280.
- SANFORD, L. P. AND M.-L. CHANG. 1997. The bottom boundary condition for suspended sediment deposition. *Journal of Coastal Research* 25:3–17.
- SANFORD, L. P. AND J. P.-Y. MAA. 2001. A unified erosion formulation for fine sediments. *Marine Geology* 179:9–23.
- SHEN, J. AND A. Y. KUO. 1999. Numerical investigation of estuarine front and its associated eddy. *Journal of Waterway, Port, Coastal, and Ocean Engineering* 125:127–135.
- SHEN, J., G. M. SISSON, A. Y. KUO, J. BOON, AND S.-C. KIM. 1998. Three-dimensional numerical modeling of the York River system, Virginia, p. 495–510. In M. L. Spaulding and A. M. Blumberg (eds.), *Proceedings of the 5th International Conference on Estuarine and Coastal Modeling*. ASCE, Reston, Virginia.
- SIMPSON, J. H., J. BROWN, J. MATTHEWS, AND G. ALLEN. 1990. Tidal straining, density currents, and stirring in the control of estuarine stratification. *Estuaries* 13:125–132.
- SISSON, G. M., J. SHEN, S.-C. KIM, J. BOON, AND A. Y. KUO. 1997. VIMS three-dimensional hydrodynamic-eutrophication model (HEM-3D): Application of the hydrodynamic model to the York River system. Special report in Applied Marine Science and Ocean Engineering No. 341. Virginia Institute of Marine Science, The College of William and Mary, Gloucester Point, Virginia.
- STACEY, M. T., S. G. MONISMITH, AND J. R. BURAU. 1999. Observations of turbulence in a partially stratified estuary. *Journal of Physical Oceanography* 29:1950–1970.
- WEIR, D. J. AND J. MCMANUS. 1987. The role of wind in generating turbidity maxima in the Tay estuary. *Continental Shelf Research* 7:1315–1318.

Received for consideration, January 16, 2002

Revised, September 26, 2002

Accepted for publication, November 18, 2002